

Bone texture analysis of human femurs using a new device (BMA™) improves failure load prediction

S. Kolta · S. Paratte · T. Amphoux · S. Persohn ·
S. Campana · W. Skalli · S. Paternotte · J.-N. Argenson ·
J.-M. Bouler · O. Gagey · C. Roux

Received: 13 October 2010 / Accepted: 9 May 2011 / Published online: 9 June 2011
© International Osteoporosis Foundation and National Osteoporosis Foundation 2011

Abstract

Summary We measured bone texture parameters of excised human femurs with a new device (BMA™). We also measured bone mineral density by DXA and investigated the performance of these parameters in the prediction of failure load. Our results suggest that bone texture parameters improve failure load prediction when added to bone mineral density.

Introduction Bone mineral density (BMD) is a strong

determinant of bone strength. However, nearly half of the fractures occur in patients with BMD which does not reach the osteoporotic threshold. In order to assess fracture risk properly, other factors are important to be taken into account such as clinical risk factors as well as macro- and microarchitecture of bone. Bone microarchitecture is usually assessed by high-resolution QCT, but this cannot be applied in routine clinical settings due to irradiation, cost and availability concerns. Texture analysis of bone has shown to be correlated to bone strength.

Methods We used a new device to get digitized X-rays of 12 excised human femurs in order to measure bone texture parameters in three different regions of interest (ROIs). We investigated the performance of these parameters in the prediction of the failure load using biomechanical tests. Texture parameters measured were the fractal dimension (Hmean), the co-occurrence matrix, and the run length matrix. We also measured bone mineral density by DXA in the same ROIs as well as in standard DXA hip regions.

Results The Spearman correlation coefficient between BMD and texture parameters measured in the same ROIs ranged from -0.05 (nonsignificant (NS)) to 0.57 ($p=0.003$). There was no correlation between Hmean and co-occurrence matrix nor Hmean and run length matrix in the same ROI ($r=-0.04$ to 0.52 , NS). Co-occurrence matrix and run length matrix in the same ROI were highly correlated ($r=0.90$ to 0.99 , $p<0.0001$). Univariate analysis with the failure load revealed significant correlation only with BMD results, not texture parameters. Multiple regression analysis showed that the best predictors of failure load were BMD, Hmean, and run length matrix at the femoral neck, as well as age and sex, with an adjusted $r^2=0.88$. Added to femoral neck BMD, Hmean and run length matrix at the femoral neck (without the effect of age and sex) improved failure load prediction (compared to femoral neck BMD alone) from adjusted $r^2=0.67$ to adjusted $r^2=0.84$.

S. Kolta · S. Paternotte · C. Roux
Rheumatology Department, Cochin Hospital,
Paris Descartes University,
Paris, France

S. Paratte · J.-N. Argenson
AP-HM, Orthopedical Surgery Department,
Sainte Marguerite Hospital, Méditerranée University,
Marseille, France

T. Amphoux
GRAFTYS,
Aix-en-Provence, France

S. Persohn · S. Campana · W. Skalli
Laboratory of Biomechanics (LBM), Arts et Métiers,
ParisTech, CNRS,
Paris, France

J.-M. Bouler
Inserm UMR 791 LIOAD, Nantes University,
Nantes, France

O. Gagey
Service du don des corps, Univ Paris-5, F-75006,
Bicêtre University Hospital, AP-HP,
Le Kremlin-Bicêtre 94270, France

S. Kolta (✉)
CEMO, Cochin Hospital,
27, Rue du Faubourg Saint Jacques,
75014 Paris, France
e-mail: sami.kolta@cch.aphp.fr

Conclusion Our results suggest that bone texture measurement improves failure load prediction when added to BMD.

Keywords Biomechanics · BMD · Bone microarchitecture · Bone texture · Failure load · Fracture

Introduction

Bone mineral density (BMD, g/cm^2) is a strong determinant of bone strength [1], but there is an overlap between BMD values of fractured and non-fractured populations [2]. Nearly half of the fractures occur in patients with BMD which does not reach the osteoporotic threshold [3]. The force in a fall is a strong risk factor that is not captured by BMD. In order to assess properly fracture risk, other factors are important to be taken into account such as clinical risk factors as well as macro- and microarchitecture of bone. Geometric parameters as hip axis length, cross-sectional moment of inertia, cortical wall thickness, and others [4] have been shown to be risk factors for fracture independent from BMD at both hip and vertebrae. Microarchitecture deterioration is actually included in the definition of osteoporosis [5]. Trabecular thickness, trabecular separation, star volume, and bone volume/trabecular volume (BV/TV) are now assessable by different techniques. Bone microarchitecture can be measured in three dimensions (3D) using high-resolution quantitative computed tomography (HR-QCT). In postmenopausal women, vertebral and non-vertebral fractures are associated with low volumetric BMD and architectural alterations of cortical and trabecular bone, measured by HR-QCT, partially independently from BMD [6]. Femoral neck QCT also provides a tool for longitudinal investigation of bone strength indices in vivo [7]. However, this technique cannot be applicable to large populations in routine clinical settings for cost and availability concerns [8]. There is a growing interest for the use of techniques with broad availability, as X-rays or bone densitometry [9, 10]. However, these projectional methods use the transformation of a 3D structure into a 2D image, and thus must be validated for bone strength analysis.

Digital radiographs can be used to provide bone texture parameters as co-occurrence matrix, run length matrix, and fractal dimension (Hmean) [11]. The fractal parameter corresponds to Hurst parameter (Hmean) and is representative of signal roughness, the co-occurrence parameter is representative of texture homogeneity, and the run length encoding parameter is representative of the number of short run length. The limitation of standard digital X-ray is the spatial resolution, which is around 4 lp/mm (pixel size, 127 μm) compared to BMA (D3A™ Medical Systems, Orléans, France) which is between 8 and 10 lp/mm (pixel size, 50 μm). This is not sufficient to visualize the smallest

trabeculae having thickness around 100 μm , where a pixel of 50 μm is needed.

Hmean, measured at the calcaneus, is able to discriminate postmenopausal women with osteoporotic vertebral fractures from age-matched controls, better than BMD alone [12]. In another study including 900 postmenopausal osteoporotic women, texture analysis of the calcaneus differentiated patients with and without prevalent vertebral fracture [13]. Fractal analysis of the calcaneus is also significantly correlated to bone strength evaluated by axial compression testing [14]. However, the calcaneus is not the best site to evaluate fracture risk as it is not a site of osteoporotic fracture, and it may not represent other bones, as the hip, precisely. It would be more relevant to directly measure bones as the proximal femur. We used a bone microarchitecture analysis (BMA) device to measure ex vivo different texture parameters: the fractal dimension (Hmean), the co-occurrence matrix, and the run length matrix at excised human femurs.

The aims of this study were:

- To compare the texture parameters at different regions of excised human femurs with the BMD at a site-matched region of interest (ROI) measured by a DXA device.
- To investigate the performance of these parameters in the prediction of the failure load using biomechanical tests.

Material and methods

Human femurs were obtained from 12 cadavers (7 women and 5 men) from donors. All cadaver femurs were obtained with legal authorization from the Department of Anatomy (Service du don des corps, Université Paris Descartes, Paris, France). Specimens were retrieved within 10 days postmortem, wrapped in saline-soaked tissues, and stored at -20°C in tightly sealed plastic bags. To exclude the presence of any focal pathology, anterior–posterior and lateral radiographs of all specimens were obtained.

Bone texture analysis

The BMA device, equipped with a 12×12 -cm detector (50 μ pixel size), was used to get the digitized anterior–posterior X-rays of these femurs. In order to standardize the acquisition technique, a ROI of 128×128 pixels was chosen in the femoral neck. The position of this ROI depends on that of two points selected by the operator. The device calculates the gray level average. If this lies within a certain range, further steps are allowed. If not, the software adapts the parameters of X-ray acquisition (kilovolt, milliamper second) and invites the operator to take another X-ray. This procedure aims at the homogenisation of the gray level

average of the X-ray and therefore allows the comparison between different X-rays. This procedure was repeated with a ROI of the same size chosen in the greater trochanter and then in the intertrochanteric region. The precision of the technique was calculated by repeating X-ray acquisition and analysis three times for ten femurs without repositioning.

The selection of the ROIs was done according to anatomical landmarks in order to be reproducible. The femoral neck ROI was chosen by positioning the two points in the middle of the upper and the lower borders of the femoral neck so that the ROI lies in the middle of the femoral neck approximately at the anatomical Ward's triangle (Fig. 1a). For the greater trochanter ROI, one point was positioned at the junction of the greater trochanter and the femoral neck, and the other, at the edge of the greater trochanter on a line perpendicular to the axis of the femur (Fig. 1b). For the intertrochanteric ROI, one point was positioned at the junction of the greater trochanter and the femoral neck, and the other, at the upper edge of the lesser trochanter (Fig. 1c). The texture parameters given by the device for each ROI are the fractal dimension (Hmean), the co-occurrence matrix, and the run length matrix.

BMD measurement

BMD of these femurs was measured on a Hologic QDR 4500A device (Hologic, Bedford, MA). They were placed in a plastic container with 14-cm-depth water in order to simulate soft tissues. Precision of the measurement was calculated by rescanning nine femurs three times without repositioning. Standard DXA femur analysis was done, and then, three ROIs were selected within the femoral neck, the greater trochanter as well as the intertrochanteric region. The size and position of these ROIs were chosen to be approximately similar to those on the BMA device.

Mechanical testing

Biomechanical testing for each femur was performed using an INSTRON 500R material testing machine by an

independent observer. Femur specimens were tested in a documented configuration simulating a fall onto the greater trochanter [15–17]. The distal third of the specimens were embedded in a metal container using a low-fusion point alloy (MCP 70; MCP Metalspecialties Inc, Fairfield, CT). It was positioned with the femoral shaft at 10° from the horizontal plane and the neck internally rotated 15°. The greater trochanter was supported by a polymeric cylinder, with possible horizontal sliding to avoid transmission of horizontal loads (Fig. 2).

The load was applied vertically on the femoral head through a PMMA spherical mold with three pre-cycles at 10 mm/min, to 0.5 mm vertical displacement, and then at 120 mm/min until failure occurred. The load–displacement curves were recorded. The fracture load (maximum load until fracture occurred) and the energy absorption (area under the curve to the point of maximum load) were calculated. For each specimen, the fracture pattern was documented and classified using the Kyle classification [18].

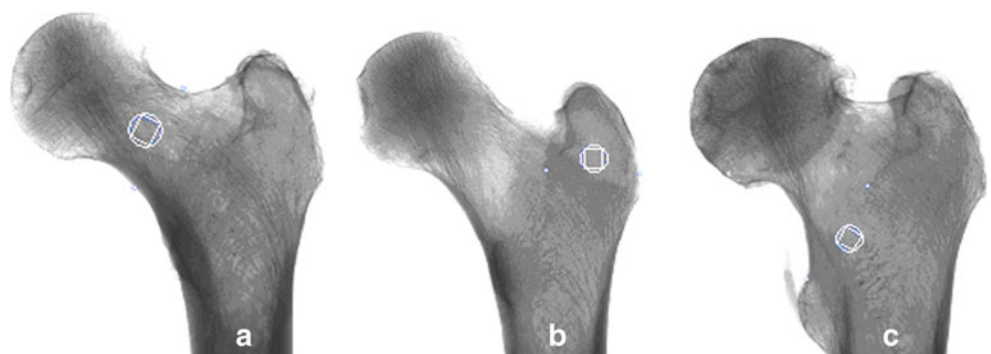
Statistical analysis

The software SAS 9.1 was used to make the statistical analysis. For the reliability analysis, intraclass coefficient correlation (ICC) with confidence interval and coefficient of variation (CV percent) were used. For the correlation analysis, the nonparametric Spearman coefficient was estimated with the *p* value of its nullity test. For the failure load predictor search, univariate and multivariate linear regressions were used.

Results

Mean age±standard deviation (SD) of the donors was 86±13 years (range, 64–101). The mean BMD±SD results of the standard DXA regions of analysis of the hip as well as of the three ROIs selected at the femoral neck, greater trochanter, and intertrochanteric region (corresponding to ROIs where BMA was measured) are presented in Table 1.

Fig. 1 Position of the three ROIs for the measurement of the BMA parameters (a femoral neck, b greater trochanter, c intertrochanteric region)



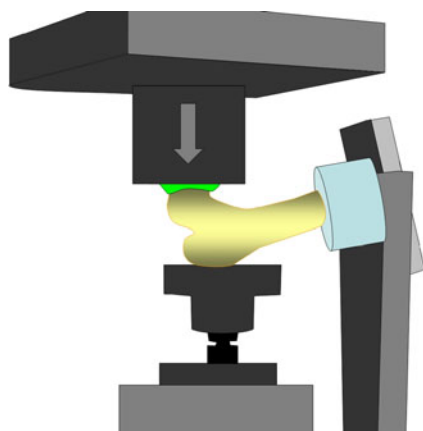


Fig. 2 Mechanical testing of a lateral stance configuration (simulation of a fall onto the greater trochanter)

Mean total hip T-score was -3.4 SD. The reproducibility of the BMA parameters is presented in Table 2. The reproducibility (CV percent) of the BMD of total hip, femoral neck, greater trochanter, and intertrochanteric regions, calculated on the same femurs, was 0.8%, 1.5%, 2.2%, and 0.9%, respectively, and that of the subregions defined on the DXA scans were 2.3%, 2.1%, and 6.4% for the subregion positioned in the femoral neck, the intertrochanteric region, and the greater trochanter, respectively.

There was no correlation between Hmean and co-occurrence matrix nor Hmean and run length matrix in the same ROI ($r=-0.04$ to 0.52 , nonsignificant (NS)). There was a strong correlation between the co-occurrence matrix and the run length matrix in the same ROI ($r=0.90$ to 0.99 , $p<0.0001$). The Spearman correlation coefficient between BMD and BMA parameters measured in the same ROIs ranged from -0.05 (NS) to 0.57 ($p=0.003$). Hmean was only significantly correlated to BMD in the same ROI at the femoral neck, not the greater trochanter nor the intertrochanteric region. The co-occurrence matrix and the run

Table 1 Mean BMD \pm SD results of the standard regions of analysis of the hip as well as of the three subregions selected at the femoral neck, greater trochanter, and intertrochanteric region (where BMA was measured)

	BMD \pm SD (min–max) (g/cm ²)
Standard hip regions	
Femoral neck	0.450 \pm 0.148 (0.234–0.662)
Greater trochanter	0.391 \pm 0.195 (0.095–0.801)
Intertrochanteric region	0.654 \pm 0.269 (0.257–1.013)
Total hip	0.544 \pm 0.225 (0.205–0.899)
Subregions	
Femoral neck	0.351 \pm 0.189 (0.011–0.643)
Greater trochanter	0.297 \pm 0.202 (0.135–0.784)
Intertrochanteric region	0.464 \pm 0.179 (0.181–0.787)

Table 2 Reproducibility of the BMA parameters evaluated by the coefficient of variation (CV) and intraclass coefficient of correlation (ICC) on ten femurs measured three times

	ICC [95% confidence interval]	Coefficients of variation (%)
Hmean		
Greater trochanter	0.47 [0.08; 0.81]	2.4
Femoral neck	0.72 [0.40; 0.91]	2.1
Intertrochanteric region	0.82 [0.59; 0.95]	1.9
Co-occurrence		
Greater trochanter	0.71 [0.40; 0.91]	1.0
Femoral neck	0.87 [0.68; 0.96]	1.7
Intertrochanteric region	0.90 [0.75; 0.97]	1.2
Run length matrix		
Greater trochanter	0.60 [0.23; 0.86]	1.3
Femoral neck	0.85 [0.63; 0.95]	2.7
Intertrochanteric region	0.87 [0.69; 0.94]	1.8

length matrix were only significantly correlated to the BMD in the same ROI of the intertrochanteric region, not the greater trochanter nor the femoral neck.

All of the fractures were Kyle II trochanteric fractures. Mean failure load (Newton) was less for women ($N=7$) compared to men ($N=5$), $1,615.00\pm 554.226$ and $2,816.60\pm 1,012.45$, respectively ($p=0.06$). Univariate analysis with the failure load revealed a significant correlation only with BMD results, not BMA ones. Results were comparable after adjustment for age and sex; $r=0.75$ to 0.82 ($p\leq 0.01$) for BMD and $r=-0.06$ to 0.54 ($p=NS$) for BMA parameters. Adjusted r^2 was 0.65, 0.67, 0.72, and 0.78 for the intertrochanteric region, the femoral neck, the total hip, and the greater trochanter, respectively ($p<0.0001$).

Multiple regression analysis showed that the best predictors of failure load were BMD, Hmean, and run length matrix at the femoral neck, as well as age and sex, with an adjusted $r^2=0.88$. Added to femoral neck BMD, Hmean and run length matrix at the femoral neck (without the effect of age and sex) improved failure load prediction (compared to femoral neck BMD alone) from adjusted $r^2=0.67$ to adjusted $r^2=0.84$.

Discussion

Our study suggests that bone texture measurement can improve the failure load prediction when added to BMD. This result is obtained in a context where BMD explains from 65% to 78% of the failure load according to the site of measurement. This is in the higher range of previously published studies using BMD measurement by DXA and biomechanical testing ($0.42<r^2<0.72$) [19–22]. BMD

results of the standard hip regions and the three subregions are within expected values of BMD in elderly, validating our measurement technique of BMD in excised human femurs. Reproducibility of our measurements (BMD and BMA) was in an acceptable range. It was assessed without repositioning because we wanted to diminish as much as possible the other sources of variation as we aimed to evaluate this new technique.

Previous clinical studies suggested that bone texture measurement can have an added value as compared to BMD. These parameters, measured at the spine [23], the femur [24], or the calcaneus [12, 25, 26], discriminated patients with and without fractures. Texture analysis of the calcaneus measured by a peripheral densitometer could differentiate between patients with and without vertebral fracture even after controlling for clinical risk factors and BMD [27]. At least two hypotheses can be drawn to explain the improvement of the failure load prediction. The first one is that, in these studies, measurements were made at different bones. Actually, using BMD, there is no evidence that adding a peripheral measurement improves the prediction value of a spine or hip measurement. This may be different for tools using different techniques, and designed to give information different than BMD, as the correlation of microarchitecture parameters measured at different sites is modest [28]. The second hypothesis of the fracture risk improvement is that bone parameters assessed by BMA and BMD measurements even at the same site are different. Previous studies comparing the fractal parameter measured on radiographs of the calcaneus to histomorphometric indices measured on biopsies of the same bone have shown that fractal parameter is correlated with trabecular separation. Furthermore, the amount of bone (evaluated by BV/TV) would explain 20% of the variance of the fractal parameter, while trabecular spacing and trabecular number explain together 38% of the variance of the fractal parameter, suggesting that fractal parameter reflects more bone microarchitecture than bone mass [29]. Fractal parameter was correlated with trabecular parameters measured by HR-pQCT at the radius and tibia, except for tibial trabecular thickness [30]. A good correlation has also been previously shown between 2D fractal dimension measured by BMA device and 3D microarchitecture using MRI images [31].

In our study, we measured BMD and texture parameters at the same site; correlations between texture parameters and BMD of the same ROI of the femur were, for most of them, nonsignificant. This is comparable to what was previously found in the calcaneus [27, 31]. It also confirms recently published results, using radiographs of 14 femurs measured in vitro: texture parameters were highly correlated with failure load (r^2 up to 0.61, $p < 0.01$) and were partially independent of BMD, suggesting that texture information contained in trabecular bone structure may determine local

bone non-quantitative parameters [32]. In another study, although site by site correlation coefficients between BMD and texture parameters in 40 excised human femurs were significant, yet BMD only partially explained texture parameters. These texture parameters performed as well as BMD measured by DXA in the explanation of failure load [33]. Texture analysis is not a direct approach of bone microarchitecture. Fractal analysis is an assessment of texture roughness and could provide structural information on the trabecular network of bone [34]. The other measurement used to characterize the texture of the bone radiography is the short run emphasis parameter (calculated from the run length matrix) where run is constituted by consecutive pixels of the same gray value in a given direction. Short run emphasis is highly dependent on the occurrence of short runs and is expected large for fine textures [35].

The precision errors of texture parameters using BMA have been previously evaluated at the calcaneus. They ranged in vivo from 1.16% to 1.24% according to the parameter [36]. In another study, Hmean measured in vivo at the calcaneus and radius was 1.2% and 2.1%, respectively. It was 4.7% at the tibia [28]. Precision errors of other texture parameters ranged from 0.5% to 3.2% for image analysis and from 1.1% to 8.3% for the entire measurement ex vivo [31]. Our study at the femur yielded comparable results (1.0% to 2.7%, Table 2).

Our study has strengths and limitations. We measured both texture parameters and BMD directly at the femur known to be a site of major osteoporotic fractures, and we used biomechanical tests to validate the texture parameters. We also measured BMD and BMA at the same site. However, our study is an exploratory one with a small number of femurs, including both genders. The effect of soft tissues on texture parameter measurement is not known.

In summary, this new technique (BMA) directly measures texture parameters which could add complementary information to BMD measurement for failure load prediction ex vivo. Further step should be in vivo studies in order to confirm that combining texture parameters of BMA to BMD would allow a better prediction of fracture risk.

Conflicts of interest None.

References

1. Marshall D, Johnell O, Wedel H (1996) Meta-analysis of how well measures of bone mineral density predict occurrence of osteoporotic fractures. *BMJ* 312:1254–1259
2. Ott SM, Kilcoyne RF, Chesnut CH (1987) Ability of four different techniques of measuring bone mass to diagnose vertebral fractures in postmenopausal women. *J Bone Miner Res* 2:201–210
3. Shuit SC, Van Der Klift M, Weel AE, De Laet CE, Burger H, Seeman E et al (2004) Fracture incidence and association with

- bone mineral density in elderly men and women: the Rotterdam study. *Bone* 34:195–202
4. Faulkner KG, Cummings SR, Black D, Palermo L, Glüer CC, Genant HK (1993) Simple measurement of femoral geometry predicts hip fracture: the study of osteoporotic fractures. *J Bone Miner Res* 8:1211–1217
 5. Christiansen C (1993) Consensus development conference: diagnosis, prophylaxis and treatment of osteoporosis. *Am J Med* 94:646–650
 6. Sornay-Rendu E, Boutry S, Munoz F, Delmas PD (2007) Alterations of cortical and trabecular architecture are associated with fractures in postmenopausal women, partially independent of decreased BMD measured by DXA: the OFELY study. *J Bone Miner Res* 22:425–433
 7. Borggrefe J, Graeff C, Nickelsen TN, Marin F, Glüer CC (2010) Quantitative computed tomographic assessment of the effects of 24 months of teriparatide treatment on 3D femoral neck bone distribution, geometry, and bone strength: results from the EUROFOR study. *J Bone Miner Res* 25:472–481
 8. Lespessailles E, Chappard C, Bonnet N, Benhamou CL (2006) Imaging techniques for evaluating bone microarchitecture. *Joint Bone Spine* 73:254–261
 9. Pothuaud L, Carceller P, Hans D (2008) Correlations between grey-level variations in 2D projection images (TBS) and 3D microarchitecture: applications in the study of human trabecular bone microarchitecture. *Bone* 42:775–787
 10. Winzenrieth R, Dufour R, Pothuaud L, Hans D (2010) A retrospective case–control study assessing the role of trabecular bone score in postmenopausal Caucasian women with osteopenia: analyzing the odds of vertebral fracture. *Calcif Tissue Int* 86:104–109
 11. Lespessailles E, Jacquet G, Harba R, Jennane R, Loussot T, Viala JF, Benhamou CL (1996) Anisotropy measurements obtained by fractal analysis of trabecular bone at the calcaneus and radius. *Rev Rhum Engl Ed* 63:337–343
 12. Pothuaud L, Lespessailles E, Harba R, Jennane R, Royant V, Eynard E, Benhamou CL (1998) Fractal analysis of trabecular bone texture on radiographs: discriminant value in postmenopausal osteoporosis. *Osteoporos Int* 8:618–625
 13. Vokes TJ, Giger ML, Chinander MR, Karrison TG, Favus MJ, Dixon LB (2006) Radiographic texture analysis of densitometric-generated calcaneus images differentiates postmenopausal women with and without fractures. *Osteoporos Int* 17:1472–1482
 14. Lespessailles E, Jullien A, Eynard E, Harba R, Jacquet G, Ildefonse JP, Ohley W, Benhamou CL (1998) Biomechanical properties of human os calcanei: relationships with bone density and fractal evaluation of bone microarchitecture. *J Biomech* 31:817–824
 15. Heini PF, Franz T, Fankhauser C, Gasser B, Ganz R (2004) Femoroplasty-augmentation of mechanical properties in the osteoporotic proximal femur: a biomechanical investigation of PMMA reinforcement in cadaver bones. *Clin Biomech* 19:506–516
 16. Beckmann J, Ferguson SJ, Gebauer M, Luering C, Gasser B, Heini P (2007) Femoroplasty-augmentation of the proximal femur with a composite bone cement—feasibility, biomechanical properties and osteosynthesis potential. *Med Eng Phys* 29:755–764
 17. Van der Steenhoven TJ, Schaasberg W, de Vries AC, Valstar ER, Nelissen RGH (2009) Augmentation with silicone stabilizes proximal femur fractures: an in vitro biomechanical study. *Clin Biomech* 24:286–290
 18. Kyle RF, Gustilo RB, Premer RF (1979) Analysis of six hundred and twenty-two intertrochanteric hip fractures. *J Bone Joint Surg* 61:216–221
 19. Cody DD, Gross GJ, Hou FJ, Spencer HJ, Goldstein SA, Fyhrie DP (1999) Femoral strength is better predicted by finite element models than QCT and DXA. *J Biomech* 32:1013–1020
 20. Lochmuller EM, Zeller JB, Kaiser D et al (1999) Correlation of femoral and lumbar DXA and calcaneal ultrasound, measured in situ with intact soft tissues, with the in vitro failure loads of the proximal femur. *Osteoporos Int* 1998(8):591–598
 21. Kukla C, Gaebler C, Pichl RW, Prokesch R, Heinze G, Heinz T (2002) Predictive geometric factors in a standardized model of femoral neck fracture. Experimental study of cadaveric human femurs. *Injury* 33:427–433
 22. Le Bras A, Kolta S, Soubrane P, Skalli W, Roux C, Mitton D (2006) Assessment of femoral neck strength by 3-dimensional x-ray absorptiometry. *J Clin Densitom* 9:425–430
 23. Caligiuri P, Giger ML, Favus Mj, Jia H, Doi K, Dixon LB (1993) Computerized radiographic analysis of osteoporosis: preliminary evaluation. *Radiology* 186:471–474
 24. Gregory JS, Stewart A, Undrill PE, Reid DM, Aspden RM (2004) Identification of hip fracture patients from radiographs using Fourier analysis of the trabecular structure: a cross-sectional study. *BMC Med Imaging* 4:4
 25. Benhamou CL, Poupon S, Lespessailles E, Loiseau S, Jennane R, Siroux V et al (2001) Fractal analysis of radiographic trabecular bone texture and bone mineral density: two complementary parameters related to osteoporotic fractures. *J Bone Miner Res* 16:697–704
 26. Lespessailles E, Gadois C, Kousignian I, Neveu JP, Fardellone P, Kolta S, Roux C, Do-Huu JP, Benhamou CL (2008) Clinical interest of bone texture analysis in osteoporosis: a case control multicenter study. *Osteoporos Int* 19:1019–1028
 27. Vokes T, Lauderdale D, Ma SL, Chinander M, Childs K, Giger M (2010) Radiographic texture analysis of densitometric calcaneal images: relationship to clinical characteristics and to bone fragility. *J Bone Miner Res* 25:56–63
 28. Cohen A, Dempster DW, Müller R, Guo XE, Nickolas TL, Liu XS et al (2010) Assessment of trabecular and cortical architecture and mechanical competence of bone by high-resolution peripheral computed tomography: comparison with transiliac bone biopsy. *Osteoporos Int* 21:263–273
 29. Lespessailles E, Roux JP, Benhamou CL, Arlot ME, Eynard E, Harba R et al (1998) Fractal analysis of bone texture on os calcis radiographs compared with trabecular microarchitecture analyzed by histomorphometry. *Calcif Tissue Int* 63:121–125
 30. Bacchetta J, Boutry S, Vilayphiou N, Fouque-Aubert A, Delmas PD, Lespessailles E et al (2010) Assessment of bone microarchitecture in chronic kidney disease: a comparison of 2D bone texture analysis and high-resolution peripheral quantitative computed tomography at the radius and tibia. *Calcif Tissue Int* 87(1):385–391
 31. Pothuaud L, Benhamou CL, Porion P, Lespessailles E, Harba R, Levitz P (2000) Fractal dimension of trabecular bone projection texture is related to three-dimensional microarchitecture. *J Bone Miner Res* 15:691–699
 32. Huber MB, Caballido-Gamio J, Fritscher K, Schubert R, Haenni M, Hengg C et al (2009) Development and testing of texture discriminators for the analysis of trabecular bone in proximal femur radiographs. *Med Phys* 36:5089–5098
 33. Chappard C, Bousson V, Bergot C, Mitton D, Marchadier A, Moser T et al (2010) Prediction of femoral fracture load: cross-sectional study of texture analysis and geometric measurements on plain radiographs versus bone mineral density. *Radiology* 255:536–543
 34. Benhamou CL, Lespessailles E, Jacquet G, Harba R, Jennane R, Loussot T et al (1994) Fractal organization of trabecular bone images on calcaneus radiographs. *J Bone Miner Res* 9:1909–1918
 35. Chappard D, Pascaretti-Grizon F, Gallois Y, Mercier P, Baslé MF, Audran M (2006) Medullar fat influences texture analysis of trabecular microarchitecture on X-ray radiographs. *Eur J Radiol* 58:404–410
 36. Lespessailles E, Gadois C, Lemineur G, Do-Huu JP, Benhamou L (2007) Bone texture analysis on direct digital radiographic images: precision study and relationship with bone mineral density at the os calcis. *Calcif Tissue Int* 80:97–102